To appear in the proceedings of IPMI 2001

The Active Elastic Model

Xenophon Papademetris[1], E. Turan Onat[2], Albert J. Sinusas[34], Donald P. Dione[4], R. Todd Constable[1] and and James S. Duncan[13]

[1] Departments of Diagnostic Radiology,
[2] Mechanical Engineering,
[3] Electrical Engineering, and
[4] Medicine, Yale University New Haven, CT 06520-8042
papad@noodle.med.yale.edu

Abstract. Continuum mechanical models have been used to regularize ill-posed problems in many applications in medical imaging analysis such as image registration and left ventricular motion estimation. In this work, we present a significant extension to the common elastic model which we call the *active elastic model*. The active elastic model is designed to reduce bias in deformation estimation and to allow the imposition of proper priors on deformation estimation problems that contain information regarding both the expected magnitude and the expected variability of the deformation to be estimated. We test this model on the problem of left ventricular deformation estimation, and present ideas for its application in image registration and brain deformation during neurosurgery.

Continuum mechanical models have been extensively used in medical imaging applications over the last ten years, particularly within the contexts of image registration and cardiac motion estimation. More recently, similar models have been applied to the problem of brain deformation during neurosurgery. The models used have been selected either (i) because of their mathematical properties (e.g. [3, 9]) or (ii) as an attempt to model the underlying physics of the situation (e.g. [11, 17, 21]). Such models are a specific case of the quadratic regularizers used in many computer vision applications, such as in the work of Horn[12] or in the deformable models used for segmentation (see McInerney and Terzopoulos [16] for a review).

The classical elastic model is derived from the properties of elastic solids such as metals. In cases of small deformations, the linear elastic model may also be applied to model biological tissue which is more hyperelastic in nature. All linear elastic models so far used in medical imaging work are *passive* models. These models will produce no deformation of their own and are essentially used for smoothing and/or interpolation. Using an elastic model results in an underestimation of the deformation as the model itself biases the estimates towards zero deformation. In this paper we present work to extend these elastic models to allow for non-zero bias. We call this model the 'active elastic model'.

The active elastic model is designed to be used to solve a problem of the following form: 'Given an input of noisy, possibly sparse, displacements find a

To appear in the proceedings of IPMI 2001

dense smooth displacement field which *results in a deformation which is close to a desired/expected deformation.*' This new method allows us to construct a proper prior model on the deformation that includes both a mean (the desired magnitude of the deformation) and a covariance (derived from the desired degree of smoothness).

The rest of this paper reads as follows: In section 1, we review the basic mathematics of the general energy minimization framework and we compare the use of a passive and an active elastic model for estimation purposes. In section 2, we examine the problem of bias in deformation estimation and demonstrate how the active model can be used to reduce this bias. We present some preliminary results of the application of an active model to reduce the bias in left ventricular deformation estimation in section 3.1 and we conclude by discussing potential applications of this methodology in other areas such as image registration and brain deformation during neurosurgery in section 4.

1 The Energy Minimization Framework

In this section we describe a framework in which the goal is to estimate a displacement field u which is a smooth approximation of a noisy displacement field u^m. We will assume that u^m is derived from some image-based algorithm, such as the shape-based tracking algorithm[20, 17], MR tagging measurements (e.g. [11]) or optical flow estimates (e.g. [12]).

We can pose this problem as an approximation problem whose solution is a least-squares fit of u to u^m subject to some smoothness constraints and takes the form:

$$\hat{u} = \underset{u}{\arg\min} \left(\int_V c(x)|u^m(x) - u(x)|^2 dv + W(\alpha, u, x) dV \right) \tag{1}$$

where: $u(x) = (u_1, u_2, u_3)$ is the vector valued displacement field defined in the region of interest V and x is the position in space, $c(x)$ is the spatially varying confidence in the measurements u^m and $W(\alpha, u, x)$ is a positive semi-definite regularization functional. W is solely a function of u, a model parameter vector α and the spatial position x.

This approach also generalizes to the case where the input displacement field u^m is *sparse*. At those locations where no measurement $u^m(x)$ exists the confidence $c(x)$ can be set equal to zero.

1.1 The Linear Elastic Model

In the early computer vision literature (e.g. [12]) the model W was generated using a regularization functional which penalized a weighted sum of the squared derivatives of the displacement field to impose a smoothness constraint. In medical imaging analysis work the classical linear elastic model is often used, especially in those cases where the problem is the estimation of a real deformation (e.g. left ventricular motion estimation [11, 17].)

A common way to define solid elastic models is in terms of an internal energy function. This internal energy function must be invariant to rigid translation and rotation in order to satisfy certain theoretical guidelines (see Eringen[8] for more details.) Hence the use of any elastic model provides no constraints on the rigid component of the displacement. Additional constraints must be employed to take advantage of any other prior information regarding the magnitude of the overall translation and rotation.

The classical linear elastic model[22] captures the mechanical properties of a deforming solid in terms of an internal, or strain energy function of the form:

$$W = \frac{1}{2}\,\epsilon^t C \epsilon \tag{2}$$

where C is a 6×6 matrix representing the elastic properties of the material and ϵ is the strain vector. In the most commonly used case, that of isotropic, infinitesimal linear elasticity these can be written as:

$$C^{-1} = \frac{1}{E}\begin{bmatrix} 1 & -\nu & -\nu & 0 & 0 & 0 \\ -\nu & 1 & -\nu & 0 & 0 & 0 \\ -\nu & -\nu & 1 & 0 & 0 & 0 \\ 0 & 0 & 0 & 2(1+\nu) & 0 & 0 \\ 0 & 0 & 0 & 0 & 2(1+\nu) & 0 \\ 0 & 0 & 0 & 0 & 0 & 2(1+\nu) \end{bmatrix}, \qquad \epsilon = \begin{bmatrix} \frac{\partial u_1}{\partial x_1} \\ \frac{\partial u_2}{\partial x_3} \\ \frac{\partial u_3}{\partial x_3} \\ \frac{\partial u_1}{\partial x_2} + \frac{\partial u_2}{\partial x_1} \\ \frac{\partial u_1}{\partial x_3} + \frac{\partial u_3}{\partial x_1} \\ \frac{\partial u_2}{\partial x_3} + \frac{\partial u_3}{\partial x_2} \end{bmatrix} \tag{3}$$

where $u(x) = (u_1(x), u_2(x), u_3(x))$ is the displacement at point $x = (x_1, x_2, x_3)$. E is the Young's modulus which is a measure of the stiffness of the material and ν is the Poisson's ratio which is a measure of the incompressibility.

In the rest of the paper we will refer to the classical linear elastic model as the *passive model* to distinguish it from the active linear elastic model described in the next section.

1.2 The Active Linear Elastic Model

The classical linear elastic model described in equation (2) is a passive model. In the absence of any external force, the material will do nothing. Given no external work, equilibrium is reached at the lowest energy state where the strain vector is identically equal to zero. Such a material model is not accurate in the case of actively deforming objects such as the left ventricle of the heart. In this case, a substantial part of the deformation is actively generated by the muscle and is clearly not a result of external forces. This active deformation does not produce a change in the strain energy of the material and to account for this factor we need to modify the elastic model appropriately. With this in mind we propose the active elastic model which takes the form:

$$W = \frac{1}{2}(\epsilon - \epsilon^a)^t C (\epsilon - \epsilon^a) \tag{4}$$

where ϵ^a is the active strain component. The active strain component represents the deformation that is not a product of external forces and hence should *not* be penalized by the model. In the absence of external forces, the active elastic model results in a deformation equal to the one actively generated by the object. So in this sense it can deform itself and hence it justifies the label *active*. Given a prior model of the active contraction, the active elastic model can also be used to generate a prediction of the position of the deforming object.

This model is also appropriate in the case where it is used to regularize an image registration problem where there is no such physical notion of active deformation. Here, the active component ϵ^a can be thought of as the expected magnitude of the deformation.

1.3 The Elastic Model as a Prior Probability Density Function

The energy minimization problem described in equation (1) can also be expressed as a Bayesian maximum a-posteriori estimation problem[17]. In this case, the solution vector $\hat{u}$ is the u that maximizes a posterior probability density $p(u|u^m)$. Using Bayes' rule, we can pose this problem (at each point x) as:

$$\begin{aligned} \hat{u} &= \underset{u}{\arg\max} \left\{ p(u|u^m) = \frac{p(u^m|u)p(u)}{p(u^m)} \right\} \\ &= \underset{u}{\arg\max} \left\{ \log p(u^m|u) + \log p(u) \right\} \end{aligned} \tag{5}$$

by noting that $p(u^m)$ is a constant once the measurements have been made.

The measurement probability $p(u^m|u)$ can be obtained by using a white noise model for the noise in the measurements u^m. The prior probability density function $p(u)$ can be derived using an energy function (such as W) using a probability density function of the Gibbs form [10]. We note that this approach has been previously used in medical imaging problems (e.g. Christensen [3], Gee [9] and others). In the cases of the passive and the active model, this prior distribution has the form:

$$\text{Passive: } \log p(u) = k_1 + \frac{-\epsilon^t C \epsilon}{2} \tag{6}$$

$$\text{Active: } \log p(u) = k_2 + \frac{-(\epsilon - \epsilon^a)^t C (\epsilon - \epsilon^a)}{2} \tag{7}$$

where k_1 and k_2 are normalization constants.

Note further that the standard multivariate normal distribution (mean=μ, covariance =Σ) has the form (k_3 is similarly a normalization constant):

$$\log p(u) = k_3 + \frac{-(u-\mu)^t \Sigma^{-1} (u-\mu)}{2} \tag{8}$$

By comparing equations (6) and (7) to equation (8), we can see that in both cases the material matrix C plays a similar role to the inverse of the covariance matrix (the stiffer the material is, the greater the coupling between the displacements of neighboring points and hence the smaller the effective component of

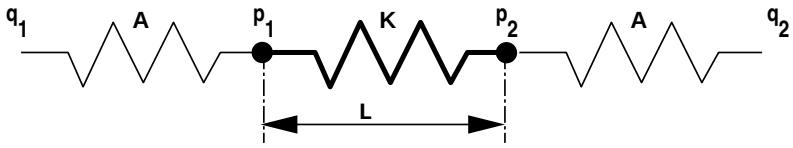

Fig. 1. A one-dimensional example. Consider a one-dimensional object consisting of two points p_1 and p_2 originally a distance L apart. The body is modeled using an elastic spring of stiffness of K. The body is then somehow deformed (stretched). In the deformed state, we have initial estimates of the positions of p_1 and p_2 shown as q_1 and q_2 respectively, and the confidence in these estimates is given by A. The problem can be visualized by connecting point pairs (p_1,q_1) and (p_2,q_2) with zero length springs of effective stiffness A and points (p_1,p_2) with a spring of stiffness K and length L. In this case, the initial displacements are given by $u^m = [q_1 - p_1, q_2 - p_2]^t$ and the strain ϵ is equal to $\frac{u_1 - u_2}{L}$.

the covariance matrix), and that in the case of the active model, the active strain ϵ^a acts like the mean of the distribution. In the case of the passive model, the mean is effectively zero. Hence we can explicitly see that the active elastic model is a generalization of the passive model, by adding the possibility of having a non-zero mean.

2 Bias Reduction Using the Active Elastic Model

The passive elastic model will likely underestimate the real deformation as a result of its penalization of all deformations. We proceed to illustrate the problem by means of a simple example and demonstrate how the active model can be used to reduce the bias. We also describe how the problem (or more precisely its symptoms) have been dealt with in the literature and point out some of the shortcomings in those approaches.

2.1 A Simple Example

To illustrate the concept of the active elastic model more concretely we will use the simple one-dimensional case described in figure 1. In this case the approximation functional (see equation 1) takes the form:

$$\hat{u} = \underset{u}{\arg\min} \left[A\Big(|u^m(p_1) - u(p_1)|^2 + |u^m(p_2) - u(p_2)|^2 \Big) + W \right] \tag{9}$$

We will consider two forms of W, a passive model W_{passive} and an active model W_{active} which have the form:

$$\begin{aligned} W_{\text{passive}} &= \frac{K}{2}\Big(\frac{u_1 - u_2}{L}\Big)^2 \\ W_{\text{active}} &= \frac{K}{2}\Big(\frac{u_1 - u_2}{L} - \epsilon^a\Big)^2 \end{aligned} \tag{10}$$

Note here that the active model reduces to the passive model if the value of the active strain ϵ^a is set to zero. Substituting for the models defined in equation (10) into equation (9), and differentiating with respect to u we obtain the following matrix equations (in the active case):

$$\begin{bmatrix} A+\frac{K}{L} & -\frac{K}{L} \\ -\frac{K}{L} & A+\frac{K}{L} \end{bmatrix} \begin{bmatrix} u_1 \\ u_2 \end{bmatrix} = \begin{bmatrix} Au_1^m + K\epsilon^a \\ Au_2^m + K\epsilon^a \end{bmatrix} \tag{11}$$

To simplify the math in order to make the illustration clearer, we set $u^m(p_2) = 0, u(p_2) = 0$. This results in the following two solutions for $u(p_1)$:[1]

$$\text{Passive Model: } u(p_1) = \frac{Au^m(p_1)}{A+\frac{K}{L}} \tag{12}$$

$$\text{Active Model: } u(p_1) = \frac{Au^m(p_1) + K\epsilon^a}{A+\frac{K}{L}} \tag{13}$$

Further we can write the expected value of $u(p_1)$, $\mathcal{E}(u(p_1))$ in terms of the expected value of $u^m(p_1)$, $\mathcal{E}(u^m(p_1))$ as:

$$\text{Passive Model} : \mathcal{E}(u(p_1)) = \Big(\frac{A}{A+\frac{K}{L}}\Big)\mathcal{E}(u^m(p_1)) \tag{14}$$

$$\text{Active Model} : \mathcal{E}(u(p_1)) = \Big(\frac{A}{A+\frac{K}{L}}\Big)\mathcal{E}(u^m(p_1)) + \Big(\frac{K\epsilon^a}{A+\frac{K}{L}}\Big) \tag{15}$$

2.2 Bias Estimation and Reduction

In the solution produced by the passive model, the expected value of $u(p_1)$ (see equation 14) will be smaller than the expected value of the measurements $u^m(p_1)$ as long as $K > 0$. Hence any estimation using the passive elastic model is *biased*, and will underestimate the actual deformation. Consider the case where $L = 1, A = 3K$. In this case by substitution into equations (14) and (15) we get the following expressions:

$$\text{Passive: } \mathcal{E}(u(p_1)) = \frac{3}{4}\,\mathcal{E}(u^m(p_1)), \qquad \text{Active: } \mathcal{E}(u(p_1)) = \frac{3}{4}\,\mathcal{E}(u^m(p_1)) + \frac{1}{4}\,\epsilon^a$$

So by an appropriate choice of ϵ^a derived from knowledge of the specific problem the bias in the estimation can be significantly reduced. For example, if we had

[1] As an aside, we also note that the expressions of equations (12) and (13) can be rewritten so that the constants K and A appear only as the ratio $\frac{K}{A}$. For example, equation (12) can be rewritten as $u(p_1) = \frac{u^m(p_1)}{1+\frac{K}{AL}}$. Hence the absolute value of the stiffness K or the data confidence A do not enter into the problem. This can be a problem in the case of the estimation of real deformation (such as in the case of the left ventricle) as the two are measured in different units and hence make the equation inconsistent from a dimensionality viewpoint.

To appear in the proceedings of IPMI 2001

prior knowledge of the expected strain in this case (where $\epsilon = \frac{u(p_2)-u(p_1)}{L}$), we could use such information to set the active strain ϵ^a so as to reduce the bias.

We note further that the effect of the bias is more significant where the relative confidence of the measurements (A) is low as a result of noisy data.

2.3 Alternative Methods of Bias Reduction

We also note that the problem of bias has been dealt with in a number of different ways in the literature (often without being actually recognized as such).

Zero Stiffness: This 'solution' is used by Park et al[19] where the Young's Modulus is set to zero. In this case, temporal filtering is used for noise reduction. This eliminates the problems associated with bias; it also forfeits all the usefulness of exploiting the spatial relationships between different points in the model. The method is successful in part because the input data are very clean.

Direct Bias Correction: Sometimes further knowledge about the problem can be used to correct for some of the bias. In our earlier work [18, 17] on left ventricular deformation estimation we solved the problem in a two step fashion, for each frame in the image sequence. At each time t the problem was solved first using a formulation like that of equation (1) to produce an estimate of the position of all the points at time $t + 1$.

Then all points that were on the endo- and epi-cardial surfaces of the heart at time t were mapped to the (pre-segmented) endo- and epi-cardial surfaces at time $t + 1$, using a modified nearest neighbor approach. In this approach the bias in the radial and circumferential directions is largely accounted for but there remains bias in the longitudinal direction (which lies parallel to the 'major' axis of the surface).

Other methods which constrain the tracked tokens to lies on a given curve or surface fall into this category of bias correction (e.g. [14]).

The Incremental Approach: In this case the estimation problem is broken into a number of small (algorithmic) steps. This has the effect of reducing the bias which is directly related to the magnitude of u^m. Consider again the simple example of figure 1 with $L = 1, A = 3K$ as before. If the displacement $u^m(p_1)$ is applied in one step, we get an estimate of $u(p_1) = 0.75u^m(p_1)$ and a bias of $0.25u^m(p_1)$.

The incremental approach is best explained algorithmically. At each increment $i \in (0, N)$ the estimate of $u(p_1)$ is defined as $d^i(p_1)$. Then, for any increment i we calculate $d^i(p_1)$ as:

$$
\begin{aligned}
&i = 0 : \;\; d^0(p_1) = 0 \\
&i > 0 : \;\; d^i(p_1) = d^{i-1}(p_1) + 0.75\Big(\frac{i}{N}\; u^m(p_i) - d^{i-1}(p_1)\Big)
\end{aligned}
$$

This essentially is a history-free approach as in each step the model is only used to regularize the difference between the current input and the last step as opposed to the whole of the input. This approach results in smaller input displacements which are closer to zero, thus resulting in a reduction of the bias. The reduction of the bias is directly related to the number of steps. In this specific case when $N = 2$ the total bias is $0.16u^m(p_1)$, when $N = 4$ it is $0.08u^m(p_1)$, and for $N = 8$, it is reduced to $0.04u^m(p_1)$.

The Fluid Model: This is essentially the limiting case of the incremental approach. In the work of Christensen[3], it takes the differential form:

$$\mu\nabla^2 v + (\lambda + \mu)\nabla(\nabla.v) = F \tag{16}$$

where F is the image derived forcing function and v is the local velocity vector. The isotropic linear elasticity model can also be written in differential form by differentiating the energy functional posed in equation (1) and generating a force F by grouping together all external displacements u^m. This takes the form (as derived in Christensen [2]):

$$\mu\nabla^2 u + (\mu + \lambda)\nabla(\nabla.u) = F \tag{17}$$

where λ and μ are the Lamè constants which are defined in terms of the Young's modulus E and the Poisson's ratio ν as[22]: $\lambda = \frac{E\nu}{(1+\nu)(1-2\nu)}$, and $\mu = \frac{E}{2(1+\nu)}$.

If we compare equations (16) with (17) we see that they have essentially the same form, with the one being in terms of the velocity v and the other in terms of the displacement u. The fluid model can be seen to be the limiting case of the incremental approach of the previous section as the step size goes to zero. This approach has the advantage of explicitly stating its assumptions properly and possibly some numerical advantages. [2]

Disadvantages of the Incremental/Fluid Approach: The incremental/fluid approach substantially reduces the bias, but the history of the deformation is lost at each (algorithmic) step. Hence in this way we cannot capture aspects of real materials such as progressive hardening with increased deformation (using non-linear elastic models) as at each step the deformation is assumed to be zero. Also the fact that the analysis is reset at the end of each step makes incorporation of temporal smoothness constraints in problems such as left ventricular motion estimation very difficult. Perhaps more fundamental in certain cases is the lack of the ability of either of these approaches to encapsulate any prior information available as to the expected magnitude of the deformation, as opposed to simply its relative smoothness.

[2] This is perhaps the answer to the 'controversy' as to whether the linear elastic model is useful in the case of large deformations. If the (passive) linear elastic model is applied using the incremental approach, as is often the case, it is really a fluid model in disguise hence it has similar large deformation capabilities.

To appear in the proceedings of IPMI 2001

2.4 Relation of the Active Elastic Model to Other Methods

In this section we clarify the relationship of certain other methods in the literature which relate or appear to relate to the active elastic model. Any criticism of these methods is simply with respect to its application in the problem of interest of our own work. (We do note that these methods were mostly designed to solve different problems.)

The thin-plate spline: A common regularization function is the thin-plate spline model[1] which in two dimensions has the form (using $u = (u_1, u_2)$ and $x = (x_1, x_2)$:

$$W(u) = \Big(\frac{\partial^2 u_1}{\partial x_1^2}\Big)^2 + \Big(\frac{\partial^2 u_1}{\partial x_2^2}\Big)^2 + \Big(\frac{\partial^2 u_1}{\partial x_1 \partial x_2}\Big)^2 + \Big(\frac{\partial^2 u_2}{\partial x_1^2}\Big)^2 + \Big(\frac{\partial^2 u_2}{\partial x_2^2}\Big)^2 + \Big(\frac{\partial^2 u_2}{\partial x_1 \partial x_2}\Big)^2$$

It can easily be shown that this function would qualify as a solid elastic model as it is invariant to rigid translation and rotation. In fact this function is invariant to all affine transformations. Hence, the bias in the estimate of the deformation in methods which utilize the thin-plate spline as a regularizer (e.g. [4]), is limited to only that component of the deformation which is not captured by an affine transform. In this respect the thin-plate spline is superior to the standard (passive) elastic regularizers, but a bias problem still remains which in certain cases could be substantial.

The Active Shape Model: In a series of papers Cootes et al (e.g. [6, 7]) presented a methodology for segmentation and registration using a point-based shape model. While this is interesting work, it does not directly relate to the active elastic model presented in this paper. The goal of the active shape model is to capture the statistical variation of the shape of a given structure/object across a number of images, whereas the goal of our work is to be able to include information regarding the expected deformation of a given object across a sequence of images.

The balloon variation of the active contour: In the balloon model of Cohen et al[5], an additional force is added to the standard snake[13] algorithm to provide for a constant expansion or contraction force. While this force does reduce the bias towards zero deformation of the underlying snake, it does so as an additional force and not as a change in the regularization model. Hence it cannot be used to capture prior information regarding the expected magnitude of the deformation, as can the elastic model.

Non-Rigid Registration of Brain Images with Tumor Pathology: Kyriacou et al [15] presented some interesting work relating to the registration of pre- and post-tumor brain images. To achieve an accurate registration a uniform contraction of the tumor is first used to estimate the shape of the post-tumor brain prior to the growth of the tumor. Unlike the balloon approach of Cohen[5], this uniform contraction procedure is very close in spirit to our work on the active elastic model, as in this case the tumor is shrinking under the influence of internal contraction and not as a result of an external force.

3 Experimental Results

3.1 Methodology

In this section we present some preliminary results of the application of this algorithm to left ventricular deformation estimation. The active elastic model is used to do two things: (i) Isovolumic Bias Correction and (ii) Imposition of a temporal smoothness constraint alongside the Isovolumic Bias Correction.

We bootstrap the algorithm by using the output produced by our previous work [18, 17]. We label this algorithm as the 'passive' algorithm. In the passive algorithm, the images are segmented interactively and then initial correspondence is established using a shape-tracking approach. A dense motion field is then estimated using a passive, transversely linear elastic model, which accounts for the fiber directions in the left ventricle. The dense motion field is in turn used to calculate the deformation of the heart wall in terms of strains. We note that, although we apply bias correction in the passive algorithm (see section 2.3) bias remains in the estimate of the strain in the longitudinal direction (which lies parallel to the 'major' axis of the surface).

The output of the 'passive' algorithm consists of a set of vectors $\epsilon^p(x_i, t_j)$ representing the strain estimated by the passive algorithm at position x_i and time t_j. Typically we divide the heart into about 800-1000 (i.e. $i \in 1:1000$) elements and use 6-9 time frames ($j \in 1:9$) resulting in a total of approximately 7000 6×1 vectors $\epsilon^p = [\epsilon^p_{rr}, \epsilon^p_{cc}, \epsilon^p_{ll}, \epsilon^p_{rc}, \epsilon^p_{rl}, \epsilon^p_{lc}]^t$. The components of ϵ^p are the normal strains in the radial (rr), circumferential (cc) and longitudinal (ll) directions as well as the shears between these direction (e.g. ϵ^p_{rc} is the radial-circumferential shear strain).

These vectors ϵ^p are then used to generate an estimate of the active strain ϵ^a (in one of two different methods as discussed below) and then a new set of output strains is estimated using the new 'active' algorithm. In this case we do not employ any additional bias correction.

A. Isovolumic Bias Correction: In this bias correction procedure at each discrete element position x_i and time t_j we generate an output vector $\epsilon^a(x_i, t_j)$ by adjusting the longitudinal strain to create a new set of strain estimates ϵ^a that result in an incompressible deformation.

The fractional change in volume produced under strain ϵ^p can be approximated as:

$$\delta V^p = (1 + \epsilon^p_{rr}) \times (1 + \epsilon^p_{cc}) \times (1 + \epsilon^p_{ll})$$

If we assume that most of the bias is in the longitudinal direction and that in reality the volume is preserved we can generate an estimate of the active strain $\epsilon^a(x_i, t_j)$ by simply (i) setting $\epsilon^a(x_i, t_j) = \epsilon^p(x_i, t_j)$ and (ii) adjusting the longitudinal component of ϵ^a to correct for any divergence from the incompressibility constraint i.e.

$$\epsilon^a_{ll} = \frac{1}{(1 + \epsilon^p_{rr}) \times (1 + \epsilon^p_{cc})}$$

These estimates ϵ^a are used as the mean value for the active elastic model. The variance is determined by the stiffness matrix and is the same as it was for the passive model. We label the results produced by this procedure as *Active*.

B. Temporal Smoothing and Isovolumic Bias Correction: In this case, before estimating the active strain component ϵ^a as above the strain vectors $\epsilon^p(x_i, t_j)$ are smoothed by performing a temporal convolution with a one-dimensional Gaussian kernel of standard deviation $\sigma = 1.0$ in the time direction to produce a temporally smooth set of vectors ϵ^s.

The ϵ^s vectors are then used instead of the un-smoothed vectors ϵ^p as the input to isovolumic bias correction procedure described above. This combined temporal smoothing and isovolumic bias correction procedure is used to generate an estimate of the active strain ϵ^a to be used with the active elastic model. We label the results produced by this procedure as *ActiveT*.

3.2 Experiments

Data: We tested the new algorithm(s) by comparing its output to those obtained using MR tagging[14] and implanted markers[18]. In the MR tagging case we used one human image sequence provided to us by Dr Jerry Prince from John Hopkins University. The images were acquired using 3 orthogonal MR tagging acquisitions and the displacements estimated using an algorithm presented in Kerwin[14]. From these displacements we estimate the MR tagging derived strains. Images from one of the three acquisitions had the evidence of the tag lines removed using morphological operators, was segmented interactively and the strains were estimated using our previous approach (Passive)[18]. In the case of implanted markers we used 8 canine image sequences with implanted markers as was described in [18].

Tests: We tested two permutations of the active algorithm. For the algorithm labeled *Active* in figure 3, we used as input the output of the *passive* algorithm after isovolumic bias correction, without any temporal smoothing. The algorithm labeled as *ActiveT* used the output of the *passive* algorithm with both temporal smoothing and isovolumic bias correction. Figure 2 illustrates the output of algorithm *ActiveT* at four points in the cardiac cycle as applied to the MR tagging sequence. The output of the tagging method[14] at End-systole is presented for comparison.

Figure 3 shows the error between the estimates of our old algorithm labeled *passive* and the two variations of the new active algorithm (*Active* and *ActiveT*), as compared to the output of the tagging algorithm[14] and to the estimates obtained using the MR markers. In the case of the tagging algorithm we observe an overall reduction in mean strain error from 9.9% (passive) to 8.1% (active) at end-systole (frame 10). In the case of the implanted markers we observe a similar reduction from 7.2% to 6.3%.

It is also interesting to note that the MR tagging algorithm [14] produces a reduction of myocardial volume of 12% between end-diastole and end-systole, our

passive algorithm an increase of approximately 14% and all both versions of the active algorithm produced small increases ($< 2\%$) showing that the isovolumic bias correction was effective.

4 Conclusions

The active elastic model is a generalization of the original elastic model which penalizes deformations away from a preset value as opposed to simply all deformations. This model can be used as a prior to solve problems where we have prior information regarding the magnitude and the variability of the expected deformation, hence it can be used to construct a proper prior probability density function for the displacement field having both a mean and a covariance, as opposed to the more traditional elastic model which has a fixed mean of zero.

The cardiac deformation example is an obvious application of this model as the active strain component can be used to model the active contraction of the left ventricle in the systolic phase of the cardiac cycle.

In the case of image registration such an active model could be used to good effect in cases where even a gross sense of the magnitude of the deformation exists a priori. For example, in Wang et al[23] where statistical shape-based segmentation information is used to constrain an elastic model, information from the segmentation regarding the relative deformation of different structures can be used with an active elastic model to drive the elastic model towards the expected solution, thus applying 'forces' to the elastic model from within as opposed to from 'the outside'.

Another example is the case of cerebro-spinal fluid loss in neurosurgery which results in large deformations in the ventricles not accounted for by gravitational forces[21]. In this case an active elastic model could be used to account for the expected large deformation of the ventricles (based perhaps on population statistics from inter-operative images) and hence reduce the bias in the final displacement field.

References

1. F. L. Bookstein. Principal warps: Thin-plate splines and the decomposition of deformations. *IEEE Transactions on Pattern Analysis and Machine Intelligence*, pages 567–585, 1989.
2. G. E. Christensen. *Deformable Shape Models for Anatomy*. Ph. D. dissertation, Washington University, Saint Louis, MI, August 1994.
3. G. E. Christensen, R. D. Rabbitt, and M. I. Miller M. I. Deformable templates using large deformation kinematics. *IEEE Transactions on Image Processing*, 5(10):1435–1447, 1996.
4. H. Chui, J. Rambo, R. Schultz, L. Win, J. Duncan, and A. Rangarajan. Registration of cortical anatomical structures via 3d robust point matching. In *Information Processing in Medical Imaging*, pages 168–181, Visegrad, Hungary, June 1999.

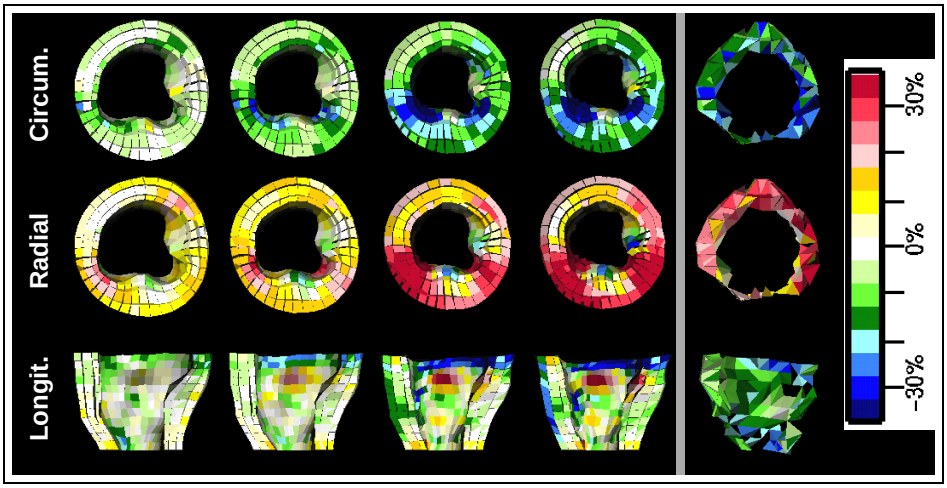

Fig. 2. *Leftmost four columns:* Circumferential, Radial and Longitudinal strain outputs of our active (*Active 2T*) algorithm at four points in the systolic half of the cardiac cycle. *Far right column:* Output of MR tagging based algorithm[14] on the same image sequence.

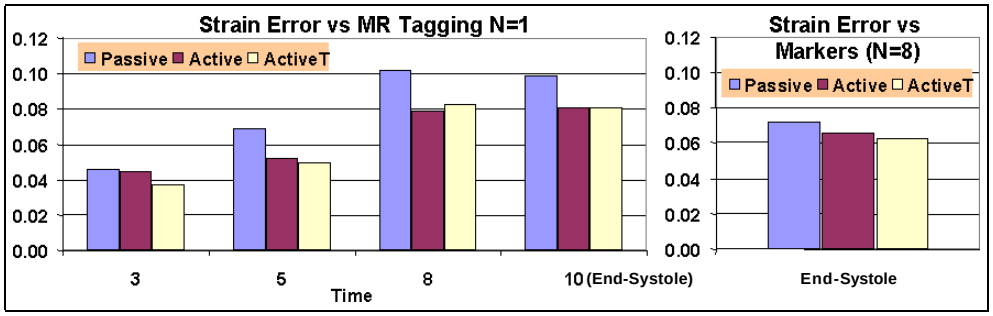

Fig. 3. Absolute Strain Error vs Tag Data or Implanter Markers. *Passive* – passive model from [18], *Active* and *ActiveT* represent two versions of the active algorithm without and with temporal smoothing. We note that both the active algorithms result in error reduction as compared to the passive algorithm. In the case of the tagging data we plot the absolute error in the cardiac-specific strains whereas in the case of implanted markers we use the principal strains instead (see [18].)

5. L. D. Cohen and I. Cohen. Finite element methods for active contour models and balloons for 2D and 3D images. *IEEE Trans. Pattern Analysis and Machine Intelligence*, 15(11):1131–1147, November 1993.
6. T. Cootes, A. Hill, C. Taylor, and J. Haslam. The use of active shape models for locating structures in medical images. In H. H. Barrett and A. F. Gmitro, editors, *Information Processing in Medical Imaging*, pages 33–47. LNCS 687, Springer-Verlag, Berlin, 1993.
7. T. F. Cootes, C. J. Taylor, D. H. Cooper, and J. Graham. Active shape models – their training and application. *Comp. Vision and Image Understanding*, 61(1):38–59, 1995.
8. A. C. Eringen. *Mechanics of Continua*. Krieger, New York, NY, 1980.
9. J. C. Gee, D. R. Haynor, L. Le Briquer, and R. K. Bajcsy. Advances in elastic matching theory and its implementation. In *CVRMed-MRCAS*, Grenoble, France, March 1997.
10. D. Geman and S. Geman. Stochastic relaxation, Gibbs distribution and Bayesian restoration of images. *IEEE Transactions on Pattern Analysis and Machine Intelligence*, 6:721–741, 1984.
11. E. Haber, D. N. Metaxas, and L. Axel. Motion analysis of the right ventricle from MRI images. In *Medical Image Computing and Computer Aided Intervention (MICCAI)*, pages 177–188, Cambridge, MA, October 1998.
12. B. K. P. Horn and B. G. Schunk. Determining optical flow. *Artificial Intelligence*, 17:185–203, 1981.
13. M. Kass, A. Witkin, and D. Terzopoulus. Snakes: Active contour models. *International Journal of Computer Vision*, 1:312–331, 1988.
14. W. S. Kerwin and J. L. Prince. Cardiac material markers from tagged MR images. *Medical Image Analysis*, 2(4):339–353, 1998.
15. S. Kyriakou and C. Davatzikos. A biomechanical model of soft tissue deformation with applications to non-rigid registration of brain image with tumor pathology. In *Medical Image Computing and Computer Assisted Intervention*, pages 531–538. Springer, Berlin, 1998. LNCS 1496.
16. T. McInerney and D. Terzopoulos. Deformable models in medical image analysis: a survey. *Medical Image Analysis*, 1(2):91–108, 1996.
17. X. Papademetris, A. J. Sinusas, D. P. Dione, and J. S. Duncan. Estimation 3D left ventricular deformation from echocardiography. *Medical Image Analysis*, in-press (March 2001).
18. X. Papademetris, A. J. Sinusas, D. P. Dione, and J. S. Duncan R. T. Constable. Estimating 3D strain from 4D cine-MRI and echocardiography: In-vivo validation. In *Medical Image Computing and Computer Aided Intervention (MICCAI)*, Pittsburgh, U.S.A., October 2000.
19. J. Park, D. N. Metaxas, and L. Axel. Analysis of left ventricular wall motion based on volumetric deformable models and MRI-SPAMM. *Medical Image Analysis*, 1(1):53–71, 1996.
20. P. Shi, A. J. Sinusas, R. T. Constable, E. Ritman, and J. S. Duncan. Point-tracked quantitative analysis of left ventricular motion from 3D image sequences. *IEEE Transactions on Medical Imaging,*, 19(1):36–50, January 2000.
21. O. Skrinjar and J. Duncan. Real time 3D brain shift compensation. In *Information Processing in Medical Imaging (IPMI 99)*, pages 42–55, 1999.
22. A. Spencer. *Continuum Mechanics*. Longman, London, 1980.
23. Y. Wang and L. H. Staib. Elastic model based non-rigid registration incorporating statistical shape information. In *Medical Image Computing and Computer Aided Intervention (MICCAI)*, pages 1162–1173. Springer, Berlin, 1998. LNCS 1496.